Journal of Materials Chemistry B

Accepted Manuscript

ROYAL SOCIETY OF CHEMISTRY

www.rsc.org/materialsB

Journal Name

RSCPublishing

ARTICLE

Self-assembly of Cytotoxic Peptide Conjugated Poly(β-amino ester)s for Synergistic Cancer Chemotherapy

Cite this: DOI: 10.1039/x0xx00000x

Received 00th January 2012,
Accepted 00th January 2012

DOI: 10.1039/x0xx00000x

www.rsc.org/

Zeng-Ying Qiao,[a,§] Chun-Yuan Hou,[a,b,§] Di Zhang,[a] Ya Liu,[c] Yao-Xin Lin,[a] Hong-Wei An,[a] Xiao-Jun Li,[b] and Hao Wang[*,a]

Nanotechnology has played an important role in cancer therapy due to the potential advantages of nano-drugs including enhanced accumulation in the tumor sites, improved pharmacokinetics and minimized systematic toxicity *in vivo*. Self-assembled peptides can improve the cellular internalization of peptides effectively through endocytosis pathway for enhanced bioavailability. Herein, cytotoxic peptide $(KLAKLAK)_2$ (named as KLAK) conjugated poly(*β*-amino ester)s (PAE-KLAK) were synthesized by Michael-type addition. The copolymers could self-assemble into micelle-like nanoparticles with pH-sensitive property, which were measured by dynamic light scattering (DLS) and transmission electron microscopy (TEM). The endocytosis pathway, mitochondria-regulated apoptosis and enhanced cytotoxicity of **P2**-KLAK micelles were proved by lysosome colocalization, JC-1 assay and CCK-8 assay in human breast cancer cells (MCF-7 cells), respectively. The cancer cell killing effect of **P2**-KLAK micelles was higher than that of free KLAK, which could be attributed to the efficient internalization into cells via endocytosis pathway and subsequent disruption of mitochondria in cells. Encapsulation of anti-cancer drug doxorubicin (DOX) into **P2**-KLAK micelles realized the co-delivery of chemotherapeutic drug and peptide drug with acid-triggered release in cells. The treatment efficacy of DOX-loaded **P2**-KLAK micelles was higher than that of DOX-loaded **P2** micelles and blank **P2**-KLAK micelles, indicating the synergistic ability to kill MCF-7 cells. Finally, *In vivo* tumor imaging and growth inhibition were evaluated in MCF-7 cell-xenografted nude mice, demonstrating that DOX-loaded **P2-**KLAK micelles could inhibit tumor growth effectively with one order magnitude lower injection amount of DOX, which was attributed to the specific accumulation in tumor sites, efficient cellular entry and controlled intracellular release of therapeutic drugs.

Introduction

Peptide drugs, classified as biopharmaceuticals or biodrugs, have attracted increasing attention as therapeutic agents in recent years.[1-6] Compared with chemotherapy drugs, peptide drugs are readily synthesized, optimized, evaluated and do not cause serious severe toxic side effects. Some of peptides with cationic amino acids are discovered as anti-tumor peptides due to their ability of targeting anionic phospholipids and disruption of negatively charged membranes.[7] An amphipathic peptide $(KLAKLAK)_2$ (named as KLAK), firstly used as antibacterial peptide, has been investigated widely. It formed α-helix with cationic amino acids on the surfaces and preferentially disrupted prokaryotic membranes and eukaryotic mitochondrial membranes rather than eukaryotic plasma membranes.[8-12] In order to increase the anti-tumor activity of the therapeutic peptides, researchers have synthesized multifunctional peptides coupled to tumor targeting ligands, which could enter targeted cells by means of receptor-mediated internalization, and subsequently induce mitochondrial-dependent apoptosis.[13-19] Other functional peptides including protein transduction domains,[20, 21] cell-penetrating peptides [22-26] and monoclonal antibodies [27] also have been applied for efficiently internalizing into cells. In addition, synthesized organic molecules such as triphenyl phosphonium cations could accumulate in the mitochondria of cells, resulting in the effective delivery of KLAK into intact cells.[28, 29]

However, the challenges in the administration of peptide drugs are i) limited hydrolytic stability and short half-life *in vivo*, ii) low bioavailability due to large molecular weight and hydrophilicity, and iii) non-targeted systemic distribution as well as other small molecular drugs.[1] To solve these problems, the peptide drugs were chemically modified to form nano-

scaled self-assembles or conjugated onto nanoparticles, which resulted in high stability and effective entrance into cancer cells. Therefore, assembled KLAK peptides were studied to improve the anti-tumor activity of free peptides *in vitro* and *in vivo*. Recently, Stupp *et al* developed a peptide amphiphilic molecule composed of hydrophilic KLAK and hydrophobic alkyl tail, which self-assembled into cylindrical nanofibers. In contrast to KLAK peptides, the self-assembled peptides were readily internalized by breast cancer cells, inducing enhanced cell cytotoxicity associated with membrane disruption.[30] To limit degradation of the peptide by the protease trypsin, pegylated peptide amphiphiles were added into the nanostructures, which had obvious antitumor activity to breast cancer *in vivo*.[31] The cytotoxic peptide amphiphiles could self-assemble into supramolecular membranes for cancer therapy, with different nanostructures varying from cylindrical nanofibers to spherical aggregates.[32] The enhanced therapy efficiency of KLAK was also realized by modifying the peptide onto inorganic nanoparticles. Ruoslahti *et al* prepared iron oxide nanoworms coated with KLAK peptide and homing peptide CGKRK, which enhances the proapoptotic activity of KLAK for glioblastoma cancer cells through both the active targeting of CGKRK and the passive targeting of nanostructures.[33] A mitochondria-targeting gold–KLAK nanoassembly was reported as effective anticancer nanomedicine.[34] Polymer carriers were also used for efficient delivery of KLAK into cancer cells through covalent conjugation and physical encapsulation.[35-37]

As a rapidly growing area of nanomedicine, polymer therapeutics can elevate therapeutic efficacy of drugs through longer retention time in the body and improved biodistribution with specific accumulation at tumor sites *via* enhanced permeability and retention (EPR) effect.[38-41] As we know, the controlled release of anticancer drugs from nanocarriers plays a vital role in the cancer treatment efficacy.[42-46] Considering the mildly acidic conditions in the intracellular compartments such as endosomes and lysosomes (pH 5–6), which are lower than that in blood circulation (pH 7.4), pH-sensitive polymers have been developed widely to realize the controlled release of loaded drugs in targeted cells.[8, 47-54] Among them, poly(*β*-amino ester)s as gene/drug carriers were first reported by Langer *et al*, which have tertiary amine groups with a pK_b value around 6.5.[55-57] PEG modified poly(*β*-amino ester)s could form nanoparticles with payloads at neutral pH due to the hydrophobicity of uncharged tertiary amine groups, and acid-triggered drug release occurred at low pH, which could be attributed to the ionization of tertiary amine and resultant increased hydrophilicity of polymer chains.[58-61] Our group have reported poly(RGD-*co*-*β*-amino ester) copolymers through the simple, reliable and one-pot synthesis method, which could kill U87 cells efficiently.[62] The drug release behaviors of pH-sensitive poly(*β*-amino ester)s in cells were monitored by photoacoustic approach.[63] Although a large number of pH-sensitive polymers were reported as chemotherapeutic drug carriers, few pH-sensitive polymers modified with therapeutic peptides were developed.

Herein, we designed cytotoxic peptide KLAK conjugated PEG-poly(*β*-amino ester)s, which were synthesized by Michael-type addition through the simple and facile synthesis method. The polymers could self-assemble into micelle-like nanoparticles with poly(*β*-amino ester)s as hydrophobic cores and PEG as hydrophilic shells (Scheme 1), which had the ability of stabilizing micelles and protecting KLAK peptide from enzyme degradation. The micelles delivered KLAK peptide into cancer cells by cellular endocytosis efficiently, which disrupted mitochondria and induced cell apoptosis more effectively than free KLAK peptide. To further elevate the antitumor activity of micelles, chemotherapeutic drug DOX was loaded into the micelles, which could release DOX at mildly acidic condition such as endosome or lysosome and kill cancer cells. The co-delivery of therapeutic peptides/chemotherapeutic drugs and their acid-triggered release resulted in the enhanced anticancer effect *in vitro* and *in vivo*, implying that the polymer nanoparticles are promising candidates for enhanced cancer therapy.

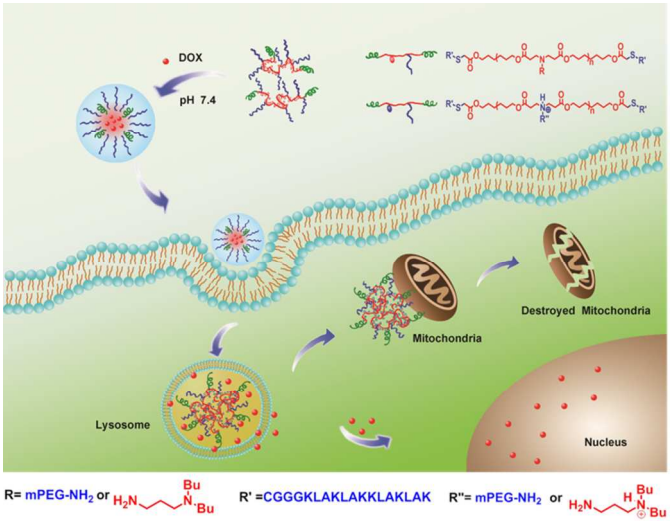

Scheme 1. DOX-encapsulated self-assembled micelle formation by cytotoxic peptide conjugated poly(β-amino ester)s and its acid-triggered release after internalization by cells for synergistic cancer chemotherapy.

Materials and methods

Materials

1,6-Hexanediol diacrylate (HDDA), 3-(Dibutylamino)-1-propylamine (DBPA), and nile red (NR) were purchased from Aldrich Chemical Corporation. Doxorubicin hydrochloride (DOX·HCl, Beijing Huafeng United Technology Co.), Methyl PEG-NH_2 2000 (Seebio Biotech, Inc.), LysoTracer Green DND-26 (Invitrogen Co.), JC-1 assay and cell counting kit-8 assay (CCK-8) (Beyotime Institute of Biothechnology, China) were used without further purification. $CGGG(KLAKLAK)_2$ peptides (>90%) were prepared using standard Fmoc solid-phase peptide synthesis methods and were purified by reverse-phase high-performance liquid chromatography (Figure S3 and S4). MCF-7 cell line was purchased from cell culture center of

Institute of Basic Medical Sciences, Chinese Academy of Medical Sciences (Beijing, China). Other solvents and reagents were used as received.

Instruments

The sizes and morphologies of copolymer micelles were measured on a DLS analyzer (Zetasizer Nano ZS) and TEM (Tecnai G2 20 S-TWIN). CD spectra of polymers and peptides were recorded using a circular dichroism spectrometer (JASCO-1500, Japan). Fluorescent measurements were performed on an F-280 fluorometer. UV-Vis spectra were recorded on a Shimadzu UV-2600 spectrometer.

Characterization of Copolymers

The chemical structures of copolymers were proved by NMR measurements. ^{1}H NMR spectra (400 MHz) of the copolymers and peptide in d^6-DMSO and D_2O containing 0.6 wt% DCl were recorded on a Bruker ARX 400 MHz spectrometer.

Synthesis of polymer-peptide conjugates

The poly(amino ester)s copolymers were prepared by Michael addition. Take **P2** as an example. HDDA (0.27 g, 1.2 mmol), DBPA (0.13 g, 0.70 mmol), mPEG-NH_2 2000 (0.60 g 0.30 mmol) were dissolved into 2 mL dimethyl sulfoxide (DMSO), and then bubbled with N_2 for 15 min under stirring. The reaction solution was heated at 50 ^{o}C for 7 days in dark and then was cooled to room temperature. The resultant solution was dialyzed against deionized water (MWCO: 3,500 Da) for 24 h and lyophilized to obtain a pale yellow solid. For the synthesis of **P2**-KLAK, CGGG(KLAKLAK)$_2$ (0.20 g, 0.11 mmol) and **P2** (0.64 g, 0.066 mmol) were added into 2 mL DMSO, and then bubbled with N_2 for 15 min under stirring. The mixture was allowed to react for 5 days at 50 ^{o}C and dialyzed against deionized water (MWCO: 3,500 Da). Other copolymers were prepared with the similar procedures.

Preparation of copolymer micelles

The copolymer micelles were prepared using the dialysis method. The copolymer (6 mg) was dissolved in 1 mL of DMSO under stirring. 2 mL of phosphate buffer (PB, 10 mM, pH 7.4) was added dropwise (50 μL/min) under constantly stirring. The solution was then dialyzed against PB (pH = 7.4) for 24 h (MWCO: 2,000 Da) to form the copolymer micelles dispersion (6 mL, 1 mg/mL).

Loading of Doxorubicin (DOX) in Micelles

The DOX-loaded copolymer micelles were prepared using the dialysis method. Take the DOX-loading experiment (Table 2, Run 2) as an example. P2-KLAK micelles (6.0 mg) and DOX·HCl (0.3 mg) were first dissolved in DMSO (1.0 mL) in the presence of excessive triethylamine (DOX/TEA in molar ratio: 1/10) to afford a free DOX solution. 2 mL PB (pH 7.4, 10 mM) was added dropwisely (50 μL/min) under constantly stirring. The resultant solution was then dialyzed against PB (pH = 7.4) for 24 h (MWCO: 2000 Da) in dark to form the DOX-loaded micelles. For calculation of the DOX loading capacity and efficiency, the micelles were dissolved by adding 50 μL of acetate buffer (pH 5.0, 5.0 M), and the dispersion volume was finally set to 6 mL (1.0 mg/mL). All the measurements were performed in triplicate in the dark. The calibration curve was obtained by a series of solutions with various DOX concentrations at 485 nm on a Shimadzu UV-2600 spectrometer in acetate buffer (pH 5.0). Then the UV-Vis spectra of dissolved solution were measured at the same measurement conditions to determine the DOX loading capacity (LC) and loading efficiency (LE). LC and LE was defined as DOX in copolymer micelles /copolymer micelles (wt%) and DOX in copolymer micelles /DOX in feed (wt%), respectively.

pH-dependent DOX Release Profiles

The release profiles of DOX from pH sensitive **P2**-KLAK micelles were obtained in the buffers of different pHs at 37 ^{o}C. Briefly, 2.0 mL of the dispersed DOX-loaded micelle dispersion (1.0 mg/mL) was added to a dialysis tubing (MWCO: 10,000 Da), which was then immersed in 10 mL buffer (PB for pH 7.4 and acetate buffer for pH 5.0, 100 mM) with shaking rate at 900 rpm. At the specific time points, 0.5 mL of the dialysis solution was taken out for the UV-Vis measurement (485 nm) and replenished with 0.5 mL fresh buffer.

Confocal laser scanning microscopy (CLSM) observation

MCF-7 cells (2×10^4 cells) were cultured in complete 1640 media at 37 ^{o}C in a humidified atmosphere containing 5% CO_2 for 24 h. For co-localization analysis, organelle specific fluorescent dyes were used. MCF-7 cells were first treated with free KLAK (45.0 μg/mL) and **P2**-KLAK micelles (167.5 μg/mL, 45.0 μg/mL for KLAK) for 1 h, 2 h and 4 h, and then washed with PBS three times. The cells were incubated with LysoTracker Green DND-26 (500 nM) for 30 minutes, and then washed with PBS three times. After replacement of medium, cells were imaged using a Zeiss LSM710 confocal laser scanning microscope with a 60× objective lens.

Mitochondria-regulated apoptosis by JC-1 assay

MCF-7 cells were cultured as above mentioned. For JC-1 assay, free KLAK (45.0 μg/mL), **P2** micelles (122.5 μg/mL) and **P2**-KLAK micelles (167.5 μg/mL, 45.0 μg/mL for KLAK and 122.5 μg/mL for **P2**) dispersed in 1640 media (2 mL) were added into cells grown in a confocal microscope dish, and the cells were further incubated at 37 ^{o}C in a humidified atmosphere containing 5% CO_2 for 12 h. The mitochondria were stained with JC-1 in 1640 medium for another 20 min. After removing the medium and washing with PBS, cells were imaged by spinning disk confocal microscopy (SDCM) observation (UltraVIEW VoX SDSM, PE Co.) with a 100× objective lens.

Cytotoxicity assay for MCF-7 cells

MCF-7 cell was utilized to evaluate the cytotoxicity of DOX-loaded **P2**-KLAK micelles by the CCK-8 assay. Free DOX,

free KLAK, **P2** micelles, **P2**-KLAK micelles, DOX-loaded **P2** micelles and DOX-loaded **P2**-KLAK micelles were dispersed in PBS (10 mM, pH 7.4) with a series of different concentrations. A density of 2×10^4 cells per well were seeded in the 96-well plates in 1640 media containing 10% FBS and 1% penicillin–streptomycin in a humidified atmosphere with 5% CO_2 and then cultured at 37 ^oC for 24 h. 10 μL of the sample solutions with different concentrations were added to each well, and the cells were incubated for additional 24 h. Then 10 μL of CCK-8 solutions was added to each well and cultured for another 4 h. The UV-Vis absorptions of sample wells (A_{sample}) and control wells ($A_{control}$) were measured using a Microplate reader at a test wavelength of 450 nm and a reference wavelength of 690 nm, respectively. Cell viability (%) was equal to ($A_{sample}/A_{control}$) x 100. All the experiments were performed in triplicate.

In vivo imaging of micelles

All animal experiments were performed complying with the NIH guidelines for the care and use of laboratory animals of Peking University Animal Study Committee's requirements and according to the protocol approved by the Institutional Animal Care. The MCF-7 cells (5×10^6 cells) collected in 1640 medium (200 μL) were transplanted subcutaneously into the rear of 6-week female BALB/c nude mice. Caliper measurements were used to estimate tumor size, and the tumor volume was calculated by equation $V=AB^2/2$, where A and B were the maximum and minimum diameters of tumors, respectively. All the tests were performed in quadruplicate. When the transplanted tumor volume reached 500 mm^3 approximately, the mice were pre-treated by 200 μL PBS or squaraines (SQ) labeled **P2**-KLAK micelles suspension (1 mg/mL) through tail vein injection. After 4 h, to acquire the whole body images, the mice were anesthetized and placed in the chamber of an *in vivo* imaging system (CRI Maestro 2). Then mice were sacrificed and the tumor, heart, liver, spleen, lung and kidney were excised for fluorescent measurement (excitation filter, 680 nm; emission filter, 726 nm).

In vivo antitumor activity

The MCF-7 cells (5×10^6 cells) were transplanted subcutaneously into the rear of 6-week female BALB/c nude mice. When the tumors reached sizes of 50-100 mm^3 (14 days after tumor cell implantation), the mice were divided into six groups (n=6) and treated via the tail vein by PBS, **P2** micelles, KLAK peptide, **P2**-KLAK micelles, DOX loaded **P2** micelles and DOX loaded **P2**-KLAK micelles (200 μL, ~0.5mg/kg for DOX, ~12 mg/kg for **P2**, ~4 mg/kg for KLAK and ~16 mg/kg for **P2**-KLAK). The drug was intravenously administered to mice on every fourth day (days 1, 5, 9 and 13). During the process of the treatment, the tumor volumes and body weight were measured every other day.

Statistical analysis

Data are presented as the mean ± standard deviation (SD). Comparison between groups was analysis with the two-tailed Student's t-test. Differences were considered statistically significant when the p values were less than 0.05 ($p < 0.05$). The level of significance was defined at $*p < 0.05$, $**p < 0.01$ and $***p < 0.001$.

Results and discussion

Synthesis and characterization of copolymers.

The poly(*β*-amino ester)s copolymers were synthesized by Michael addition of hydrophobic monomer HDDA, pH-sensitive monomer DBPA and hydrophilic PEG-NH_2 (Scheme 2), which formed the amphiphilic pH-sensitive graft copolymers with self-assembly property. The chemical structures of copolymers with acrylate groups at the both ends of copolymer chains were proved by ^1H NMR spectra (Fig. 1a and Fig. S1). The molar ratio of HDDA to DBPA and mPEG-NH_2 in feed was 1.1:1, 1.2:1 and 1.3:1, obtaining graft copolymers **P1**, **P2** and **P3**, respectively. The degree of polymerization (DP) and molecular weight (M_W) of copolymers were controlled by varying the excess ratio of HDDA, which could be determined by ^1H NMR spectra (Table 1, Fig. 1a and Fig. S1). For copolymer **P1**-**P3**, the area of peak 10 at ~4.0 ppm and peaks at 5.8~6.3 ppm belonging to the acrylate end group were used for calculating the DP of copolymers. The DP value of **P1**, **P2** and **P3** was 12, 9 and 5, respectively. Similarly, the peak of PEG at ~3.5 ppm and peak 1 of DBPA at ~0.8 ppm were utilized for calculating the molar ratio of PEG chains to DBPA monomers, and the molar fractions of PEG in copolymer chains (~33%) were similar with the feed ratio of PEG (30%). Hence, M_W of copolymers could be determined by the DP value and the molar ratio of PEG to DBPA. The copolymers with higher M_W were gained by lowering the excess amount of HDDA, which was in accordance with the principle of condensation polymerization and reported Poly(*β*-amino ester)s copolymers.[64, 65] To obtain KLAK peptide conjugated poly(*β*-

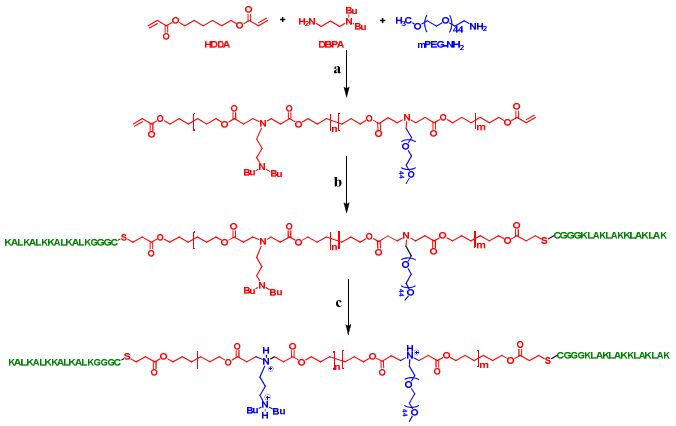

Scheme 2. Synthesis route and acid-triggered ionization of KLAK conjugated poly(β-amino ester)s copolymer. (a)Michael addition, DMSO, 50 ^oC, 7 d. (b) $CGGG(KLAKLAK)_2$, Michael addition, DMSO, 50 ^oC, 5 d. (c) H_2O/H^+

Table 1. Characterization and aggregation properties of the copolymers [a]

Polymer	HDDA:DBPA:PEG-NH_2 [b]	M_W [c]	D_{h1} [d] (nm)	PDI [d]	D_{h2} [e] (nm)	D_{h2} [f] (nm)	Zeta Potential [g] (mV)
P1	1.1:0.7:0.3	10800	55.5 (99.5%) 264 (0.5%)	0.55	N/A	53.5 (99.5%) 253 (0.5%)	0.22
P2	1.2:0.7:0.3	9600	34.1	0.17	219	37.1	0.97
P2-KLAK	1.2:0.7:0.3	13200	18.5	0.18	285	15.6	5.34
P3	1.3:0.7:0.3	4300	116	0.35	N/A	139	0.12

[a] Copolymerization conditions: Michael addition, DMSO, 50 °C. [b] Molar feed ratio. [c] Molecular weight of copolymers determined by ^{1}H NMR spectra. [d] Average hydrodynamic diameter and dispersity index measured by DLS for the copolymer micelle dispersions (pH 7.4, 10 mM PB). [e] Average hydrodynamic diameter measured by DLS for the copolymer micelle dispersions (pH 5.0, 50 mM acetate buffer solution). [f] Average hydrodynamic diameter measured by DLS for the copolymer micelle dispersions (pH 7.4, 10 mM PBS) after 24 h. [g] Zeta potential measured by DLS for the copolymer micelle dispersions (pH 7.4, 10 mM PB).

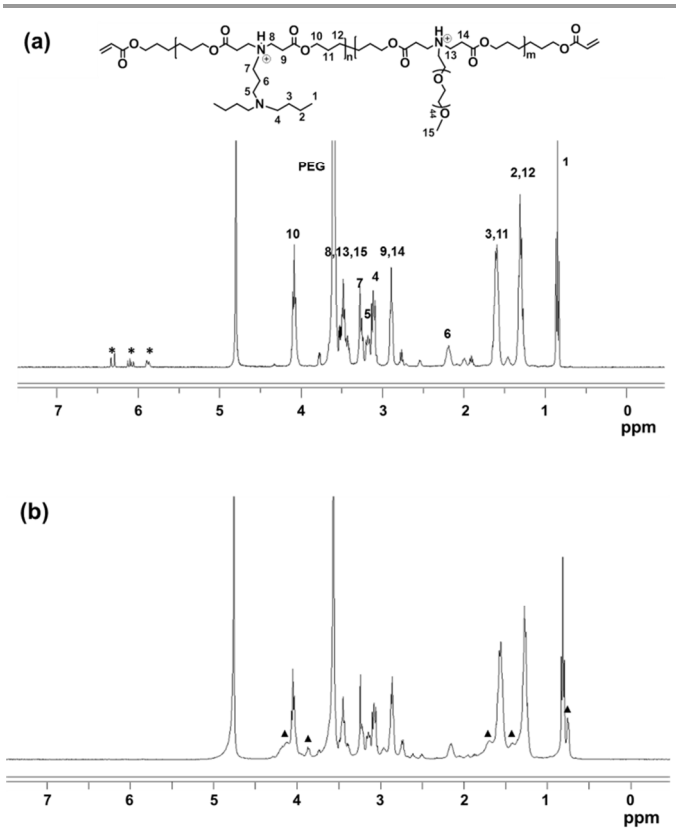

Fig. 1. ^{1}H NMR spectra of poly(*6*-amino ester)s copolymers **P2** (a) and **P2**-KLAK (b) in D_2O containing 0.6 wt% DCl. Asterisks (*) represent the double bonds of acrylate end groups. The KLAK peptide signals are denoted by black triangles.

amino ester)s copolymers, the peptide $CGGG(KLAKLAK)_2$ was synthesized with thiol group at one end (Scheme 1). The reaction activity of thiol groups was much higher than that of primary amino groups, ensuring that the amino groups in KLAK peptide did not participate in the reaction. The ^{1}H NMR spectrum of **P2**-KLAK indicated that the acrylate groups were reacted totally and KLAK peptides were linked on the both ends of copolymer chains due to the disappearance of peak at 5.8~6.3 ppm and the appearance of KLAK peaks by contrasting the spectra of KLAK and **P2**-KLAK (Fig. 1b and Fig. S2).

Self-assembly of copolymers in aqueous solution

At pH 7.4, the copolymers containing hydrophobic HDDA and DBPA could self-assemble into micelle-like nanoparticles due to the deionization of tertiary amine groups. The copolymer backbone composed by DBPA and HDDA constituted the hydrophobic core, while PEG side chains formed the hydrophilic shell. The hydrodynamic diameters (D_h) of micelles were measured by DLS, indicating that micelles with different sizes were prepared by the copolymers with various compositions (Table 1). However, large sizes and PDI values were observed for **P1** and **P3**, proving that the copolymers could not be applied as drug nanocarriers. Therefore, **P2** was the optimal copolymers for further conjugation of KLAK peptide, which was attributed to the suitable micelle size and high incubation stability of **P2** micelles. As shown in Table 1 and Fig. 2a, the diameter of **P2**-KLAK was smaller than that of **P2**. We speculated that the hydrophilic fractions of copolymers were increased by KLAK peptide resulting in the formation of micelles with smaller sizes. Considering the protection effect of PEG, Zeta potential of **P2**-KLAK was measured with the value of around zero, indicating that PEG chains could totally shield electropositive KLAK. The high stability of **P2**-KLAK micelles in PBS after 24 h also proved the potential application of the micelles as nano-drugs *in vivo*. The morphologies and sizes of the copolymer micelles were also observed by TEM, showing that **P2** and **P2**-KLAK micelles were almost spherical with an average size of 32±3 nm and 22±8 nm, respectively, which was in accordance with the results of DLS (Fig. 2c and 2d). To ensure the KLAK conjugation on copolymer chains with intact structures, the circular dichroism (CD) spectra of KLAK peptide and **P2**-KLAK micelles were investigated using standard CONTINLL algorithms.[66, 67] Compared to KLAK peptide with 80.2% α-helical structure, **P2**-KLAK micelles remained 55.2% α-helical structure, proving that 69% of the secondary structure of KLAK peptide was not destroyed during the process of copolymer synthesis and nanoparticle preparation (Fig. 2b).

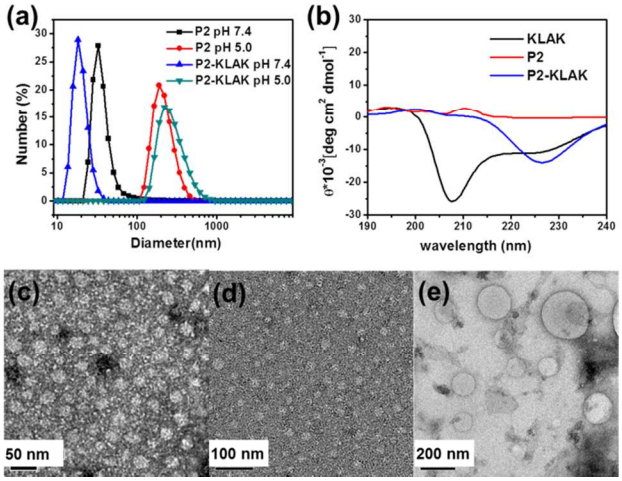

Fig. 2. (a) Number size distribution of micelles (1.0 mg/mL) in PB solutions (10 mM, pH 7.4) and acetate buffer (50mM, pH 5.0) measured by DLS. (b) CD spectra of **P2** micelle, **P2**-KLAK micelle and KLAK peptide in PB solution (10 mM, pH 7.4). TEM images of **P2** (c) and **P2**-KLAK (d) in aqueous solutions at pH 7.4. (e) TEM images of and **P2**-KLAK in aqueous solutions at pH 5.0.

pH-sensitive properties of copolymer micelles

Similarly with other poly(*β*-amino ester)s copolymers reported before, these copolymers are also pH-sensitive due to the reversible protonation of tertiary amine groups. Fluorescence spectroscopy using pyrene as a probe was measured to determine the pK_b value of copolymers.[68] The ratios of I_{338}/I_{333} at various pHs were calculated as indexes of micelles hydrophobicity. The ratio of I_{338}/I_{333} did not show obvious change at pH 5~5.6, implying that no obvious hydrophobic microdomains existed due to the protonated tertiary amine groups of copolymers (Fig. 3a). At pH 5.6, there was an increase of the ratio of I_{338}/I_{333}, implying the formation of core-shell micelles above this pH because of the deprotonated amine groups. The enhanced I_{338}/I_{333} values at pH 6.8 indicated that the copolymers formed stable micelles in extracellular circumstances, which was important for intracellular controlled release of therapeutic drugs.

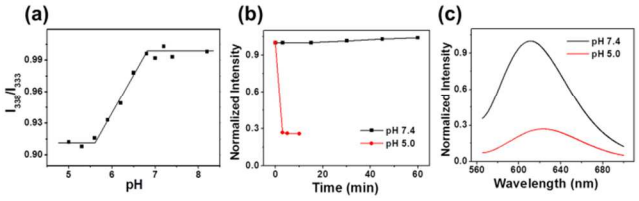

Fig. 3. (a) I_{338}/I_{333} ratio of pyrene vs pH value determined by fluorescence spectrometer in **P2**-KLAK aqueous solution (10 mM PB). (b) Incubation time-dependent change of the normalized fluorescence intensity of NR in **P2**-KLAK micelle dispersions at different pHs. (c) pH-dependent fluorescence spectra of NR in micelle dispersions.

The acid-triggered dissociation behaviors of copolymer micelles were investigated by DLS in aqueous solutions of pH 5.0. The stable **P2** and **P2**-KLAK copolymer micelles formed at neutral pH with diameter of 18-34 nm, and the nanoaggregates with sizes larger than 200 nm were observed at acidic pH, which were proved by DLS (Table 1 and Fig. 2a). The larger nanoparticles of 203±66 nm at pH 5.0 were also observed by TEM images, further proving the increased size of ionized copolymer aggregates (Fig. 2e and S5). For most pH-sensitive polymers, the protonated tertiary amines and increased hydrophilicity of polymer chains at low pH could result in the dissociation of polymer nanoparticles with the decrease of diameter. However, the larger sizes of aggregates were measured for these copolymers, which may be attributed to the remnant hydrophobicity of HDDA units and the hydrogen bonding between copolymers chains, resulting in the swelling of copolymer micelles and subsequent intermicellar aggregation. The similar phenomena were also reported by literatures.[60, 69, 70]

Considering that no single chains were observed at acidic condition, the release behaviors of guest molecules from copolymer micelles must be ensured. Nile red (NR), which is a polarity-sensitive hydrophobic dye, can be applied as a model hydrophobic probe for fluorescence measurement.[71, 72] At pH 7.4, NR probes were encapsulated in the hydrophobic cores of **P2**-KLAK copolymer micelles, showing strong fluorescence because of the relatively nonpolar microenvironment (Fig. 3b and 3c). The fluorescence intensity of micelle dispersions exhibited no obvious changes in 60 min at neutral pH, indicating that the copolymer micelles were stable at this time scale. When the pH decreased to 5.0, the NR emission intensity decreased rapidly in 3 min, which is reasonable due to the fast ionization of copolymer chains and subsequent disappearance of the NR located hydrophobic microdomains, releasing NR molecules in aqueous solutions with low fluorescence quantum yield. Interestingly, still ~26% of the initial NR intensity value was measured after acid-triggered dissociation, implying that part of NR remained in some kind of hydrophobic microdomains. We speculated that the hydrophobic HDDA units may cause further aggregation after micelles dissociation, adsorbing or encapsulating some NR molecules, which was in accordance with DLS results.

NR is known as a solvatochromic dye with a red-shift of the maximum emission wavelength (λ_{max}) while the solvent polarity increases.[73] NR is also a solvatochromic dye, the maximum emission wavelength (max) of which red-shifts as the solvent polarity increases. For **P2**-KLAK micelles, λ_{max} of NR was ~611 nm at pH 7.4, indicating that NR were loaded in the hydrophobic cores of micelles (Fig. 3c). At pH 5.0, the λ_{max} of emission spectrum occurred red-shifting to ~623 nm, which could be attributed to the dissociation of micelles and resultant polarity increase of the NR microenvironment. However, the λ_{max} of dissociated copolymers (~623 nm) was lower than that of our reported copolymers before (~640 nm), implying that the existence of nanoaggregates with more hydrophobic microdomains,[62, 63] which was in agreement with the formation of large aggregates observed by DLS. Therefore, the copolymer micelles were stable in physiological environment and could release the therapeutic drugs quickly at weakly acidic condition of lysosome after entering into cells.

Cytotoxicity and cellular internalization of copolymer micelles

In order to investigate the self-assembly effect of KLAK peptide toward cancer cells, **P2**-KLAK micelles were compared with free KLAK peptide and blank **P2** micelles for cytotoxicity assay. As shown in Fig. 4, **P2** and KLAK peptide did not display obvious cytotoxicity at a concentration up to 245 μg/mL and 90 μg/mL, respectively. However, compared with KLAK peptide, the **P2**-KLAK micelles showed enhanced cytotoxicity at a concentration of 9 μg/mL (for KLAK), and lower cell viability was measured upon increasing the KLAK concentration, indicating that they could kill the MCF-7 cancer cells effectively. Compared with KLAK peptide (IC_{50} ~890 μg/mL, Fig. S6), IC_{50} of **P2**-KLAK micelle was reduced to ~50 μg/mL, exhibiting enhanced anticancer ability by ~18 times.

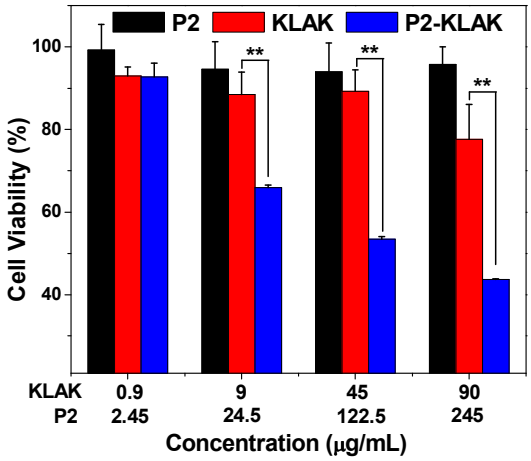

Fig. 4. MCF-7 cell viability incubated with **P2**, KLAK and **P2**-KLAK measured by the CCK-8 assay. Results are presented as the mean ± SD in triplicate. Asterisks (*) denoted statistical significance; Statistical significance: **p< 0.01.

The enhanced anti-cancer effect of **P2**-KLAK micelles compared with free KLAK peptide may be relative to the different cell uptake processes. The subcellular localization of KLAK and micelles labeled with Cy5 in MCF-7 cells was measured by confocal laser scanning microscopy observation, and the lysosomes of cells were stained by LysoTracker Green DND-26. As shown in Fig. 5 and S7, free KLAK peptide could not enter into cells efficiently in 4 h, which was a common phenomenon for peptide drugs, resulting in the low cytotoxicity to cancer cells. However, **P2**-KLAK micelles could enter into cells by endocytosis pathway in 1 h, proved by the colocalization of micelles and lysosomes. With the increase of incubation time, the fluorescence intensity of Cy5 increased gradually due to the accumulation of micelles in cells. Additionally, Poly(*β*-amino ester)s is known to induce endosomolysis within the cytoplasm through "proton sponge" effect,[74] so the micelles can be released from acidic lysosomes into the cytoplasm, which was verified by lysosome colocalization. At 4 h, a part of micelles escaped from lysosome, avoiding the peptide degradation and ensuring the further interaction with mitochondria.

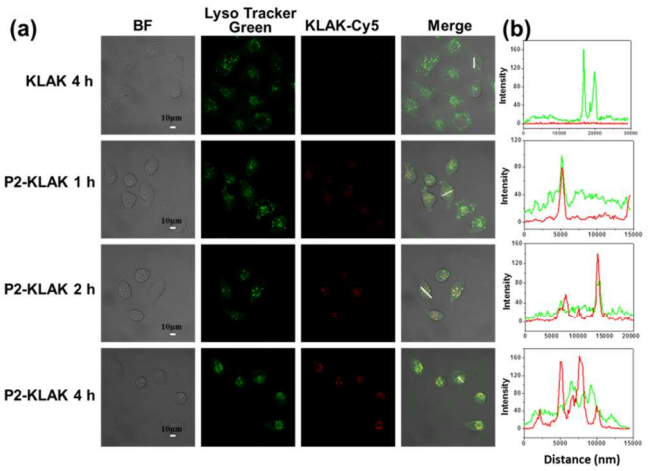

Fig. 5. (a) CLSM microscopy of living MCF-7 cells that were incubated with KLAK peptide for 4 h and **P2**-KLAK for 1 h, 2 h, 4 h, respectively. KLAK concentration: 45 μg/mL. Lysosomes were labeled with LysoTracker Green DND-26 for 30 min before imaging. (b) Representative line pot of MCF-7 cells, and the according fluorescence signals distribution based on the white line in merge images.

As above mentioned, KLAK could kill cancer cells by disrupting mitochondrial membranes, so JC-1 assay was applied for studying the process of cell apoptosis (Fig. 6). For free KLAK and **P2** micelles, the green JC-1 monomer aggregated in the normal mitochondria with the formation of red *J*-aggregate, which was similar to the control cells without any treatment, indicating that both free KLAK and **P2** micelles could not induce the cell death. In contrast, for **P2**-KLAK micelles similarly with positive control CCCP, the red fluorescence nearly disappeared with the increase of green fluorescence, illustrating that the mitochondria were destroyed seriously. Therefore, the **P2**-KLAK micelles could enter cells by endocytosis pathway, escape from lysosome and disrupt mitochondria in cells more effectively than free KLAK, causing the higher cytotoxicity.

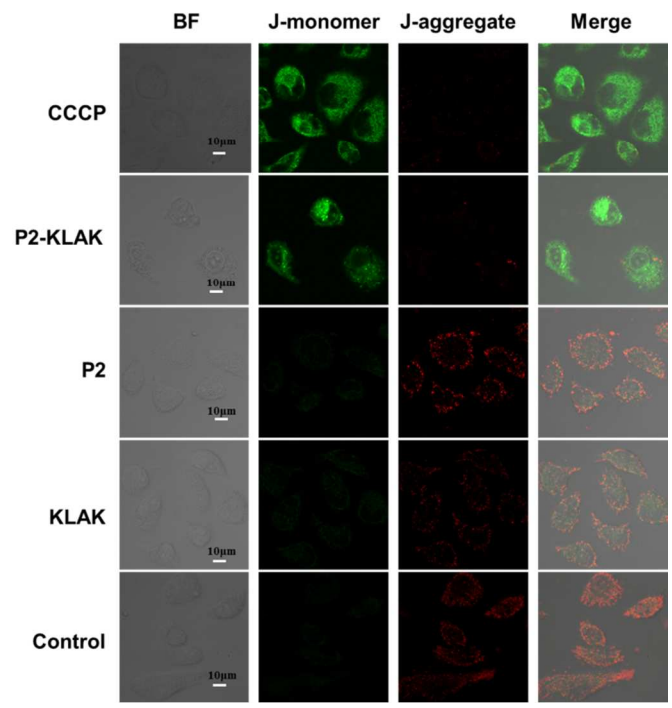

Fig. 6. Comparison of mitochondrial membrane potentials (JC-1 assay) in MCF-7 cells after incubation with **P2**, KLAK, and **P2**-KLAK for 12 h with KLAK concentration at 45 μg/mL.

DOX loading and acid-triggered release

Due to the formation of copolymer micelles at pH 7.4, the hydrophobic anti-cancer drugs could be encapsulated into the cores of **P2**-KLAK micelles for enhanced cancer therapy. Free DOX was loaded **P2** and **P2**-KLAK micelles with loading capacity of 4.14% and 3.76%, respectively (Table 2). The loading capacity of **P2**-KLAK micelles was lower than that of **P2** micelles, which could be attributed to the low hydrophobic fraction of **P2**-KLAK. The diameters of DOX-loaded micelles were measured by DLS, which were larger than that of blank micelles due to the hydrophobicity of DOX (Table 2 and Fig. 7a). However, the sizes of nanoparticles were still below 100 nm, which was suitable for optimized *in vivo* distribution and cellular internalization as anticancer drug carriers.[75] To demonstrate that the micelles are suitable for intravenous injection with long circulation stability, the size changes of the DOX-loaded **P2**-KLAK micelles in PBS solutions was evaluated by DLS (Fig. 7b). Little change of micelle diameter was observed within 5 h, proving the good incubation stability of the DOX-loaded micelles, which had great potential as nano-drugs for systemic administration.

Table 2. Loading capacity and efficiency of DOX-loaded copolymer micelles [a]

Run	Polymer	HDDA:DBPA :mPEG-NH_2 [b]	w_d/w_p (wt %)	LC (wt %) [c]	LE (wt %) [d]	D_h (nm) [e]
1	P2	1.2:0.7:0.3	5	4.14±0.12	82.8±2.4	63.8
2	P2-KLAK	1.2:0.7:0.3	5	3.76±0.16	75.2±3.2	27.3

[a] DOX loading experiments were performed in PB (pH 7.4, 10 mM). [b] w_d/w_p denotes the initial drug/polymer ratio in feed. [c] Loading capacity (LC) is defined as the percent ratio of drugs in polymer micelles/polymer micelles. [d] Loading efficiency (LE) is defined as the percent ratio of drugs in polymer micelles/drugs in feed. [e] Average hydrodynamic diameter measured by DLS for the copolymer micelle dispersions (pH 7.4, 10 mM PB).

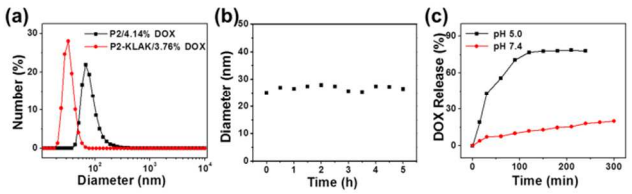

Fig. 7. (A) Number size distribution of DOX-loaded micelles in 10 mM PB solutions (pH 7.4) measured by DLS. (B) Hydrodynamic diameter vs time plots of **P2**-KLAK micelles loaded with DOX in PBS solution (10 mM, pH 7.4) at 37 °C. Copolymer concentration: 1.0 mg/mL. (c) *In vitro* cumulative release profiles of DOX from **P2**-KLAK micelles at different pHs.

The *in vitro* acid-triggered DOX release profiles from micelles were investigated by a dialysis method using the UV-Vis spectroscopy to quantify the released DOX (Fig. 7c). The cumulative release of DOX from **P2**-KLAK micelles at pH 7.4 was only ~20% in 300 min, suggesting a satisfactory stability of the DOX-loaded micelles at physiological condition. In contrast, the DOX release was significantly accelerated at pH 5.0 with ~80% release amount in 100 min, which was in accordance with the release behavior of NR from micelles.

Enhanced anti-cancer efficacy of DOX-loaded P2-KLAK micelles

The cytotoxicity of free DOX, DOX-loaded **P2** micelles, **P2**-KLAK micelles and DOX-loaded **P2**-KLAK micelles were evaluated by CCK-8 assay in MCF-7 cells (Fig. 8). At a concentration of 0.1 μg/mL for DOX and 0.9 μg/mL for KLAK, both DOX-loaded **P2** micelles and **P2**-KLAK micelles did not show obvious cytotoxicity to cell. However, only ~56% of cell viability was measured for DOX-loaded **P2** micelles, indicating the synergic effect of DOX and self-assembled KLAK at low concentration. As the concentration of DOX and KLAK increased, DOX-loaded **P2**-KLAK micelles still showed lowest cell viability, which showed enhanced anti-cancer efficacy to MCF-7 cells. The cellular endocytosis pathway of DOX-loaded **P2**-KLAK micelles was also observed by the colocalization of DOX-loaded micelles and lysosomes (Fig. S8). As we know, DOX could induce cell death by entering cellular

nucleus and inserting the base pairs in DNA, and KLAK peptides kill cancer cells by disrupting mitochondria. We speculated that the different anticancer mechanisms resulted in the synergistic effect of peptide and DOX, which destroyed mitochondria and cellular nucleus simultaneously, inducing cell apoptosis effectively at low concentration.

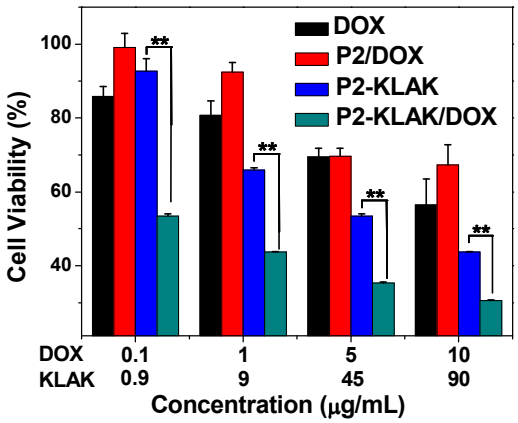

Fig. 8. MCF-7 cell viability incubated with DOX, **P2**/DOX, **P2**-KLAK and **P2**-KLAK/DOX measured by the CCK-8 assay. Results are presented as the mean ±SD in triplicate. Asterisks (*) denoted statistical significance; Statistical significance: **p< 0.01

In vivo imaging and anti-tumor effect of micelles

To monitor the biodistribution of **P2**-KLAK micelles in MCF-7 tumor xenografted mice, a near-infrared (NIR) fluorescent probe squaraine (SQ) dye was incorporated into the micelles, which displayed a maximum absorption peak at 680 nm and a fluorescent emission peak at 726 nm.[45, 46, 76] SQ loaded **P2**-KLAK micelles were injected into MCF-7 tumor-bearing nude mice through the tail vein. Mice treated with intravenous injection of PBS were used as control. Strong fluorescent signals around tumor were observed after 4 h injection (Fig. S9), indicating the specific tumor targeting of **P2**-KLAK micelles by EPR effect. The biodistribution of **P2**-KLAK micelles in mice was further evaluated by *ex vivo* experiments. As shown in Fig. 9a and 9b, after 4 h post injection, the tumor exhibited stronger signal than other harvested organs, *i.e.*, spleen, lung, heart and kidney except for liver. The high tumor accumulation of polymer micelles and acid-triggered release of drugs implied the enhanced therapeutic efficacy *in vivo*.

MCF-7 cancer cells xenografted tumor nude mice model was utilized for evaluate the *in vivo* tumor suppression effect of DOX-loaded **P2**-KLAK micelles. The process of tumor growth was observed for 15 days, and tumor inhibition efficacy of different groups, i.e., PBS, **P2** micelles, KLAK peptide, **P2**-KLAK micelles, DOX loaded **P2** micelles and DOX loaded **P2**-KLAK micelles were summarized as plots of tumor volumes over the treatment time. As shown in Fig. 9c, the tumors treated with **P2**-KLAK micelles increased more slowly than that of KLAK peptides. It was reasonable that the free KLAK peptides were degraded and removed from body quickly, and hence few KLAK could play a role on the tumor treatment. However, nano-scaled **P2**-KLAK micelles could specifically cumulate into the tumor site by EPR effect with controlled release behaviors, exhibiting effective anti-tumor ability. Furthermore, DOX loaded **P2**-KLAK micelles could suppress the tumor growth more significantly than **P2**-KLAK micelles and DOX loaded **P2** micelles, showing possible synergic cancer treatment effect. As we know, DOX with concentration of 5~10 mg/kg was usually used for treating tumor, which also appeared significant toxicity *in vivo*. In this drug delivery system, only 0.5 mg/kg of DOX was injected into mice, and the bodyweight of the mice treated with DOX loaded **P2**-KLAK micelles revealed slight increase from 20.6 g to 22.6 g (Fig. 9d), proving little toxicity of encapsulated DOX. Therefore, the significant tumor suppression effect of DOX loaded **P2**-KLAK micelle was realized without obvious toxic side effect.

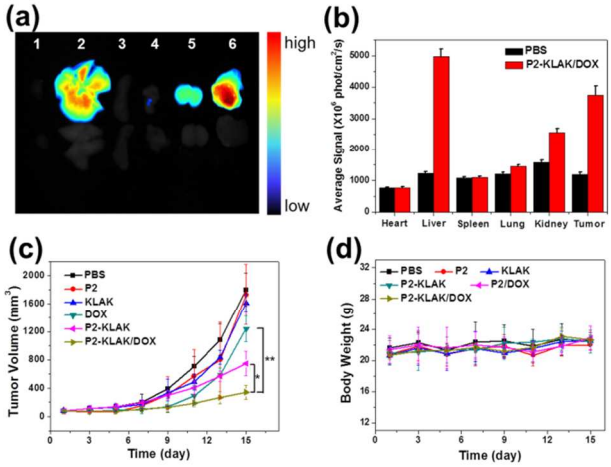

Fig. 9. (a) *Ex vivo* NIR optical imaging of tissues and tumors at 4 h after intravenous administration of SQ loaded **P2**-KLAK micelles (above) or PBS (below); 1. Heart; 2. Liver; 3. Spleen; 4. Lung; 5. Kidney; 6. Tumor. (b) Quantitative analysis for the biodistribution of SQ loaded **P2**-KLAK micelles in major organs 4 h post-injection to mice. Mice treated with PBS were regarded as the control group. Each column represented the mean value (n=3). Data were represented as means ±S.D. (c) Tumor volume changes after intravenous injection of PBS, **P2** micelles, KLAK peptide, **P2**-KLAK micelles, DOX loaded **P2** micelles and DOX loaded **P2**-KLAK micelles in MCF-7 tumor-bearing nude mice. (d) Body weight changes of the six groups over the course of treatments. Values were expressed as means ±S.D. (N=6). Asterisks (*) denoted statistical significance; Statistical significance: *p <0.05, **p< 0.01 and ***p < 0.001.

Conclusions

The KLAK peptide conjugated poly(*β*-amino ester)s were prepared by Michael-type addition, which self-assembled into micelle-like nanoparticles at neutral pH. The **P2**-KLAK micelles displayed enhanced cytotoxicity to MCF-7 cells, which could be attributed to efficient internalization of KLAK peptide into cells by endocytosis pathway and subsequent disruption of mitochondrial membranes. The micelles could encapsulate anti-cancer drugs DOX in hydrophobic cores, and acid-triggered drug release occurred at mildly acidic condition due to the ionization of tertiary amines. Therefore, co-delivery of self-assembled KLAK peptide and DOX realized synergistic

cancer treatment with increased cytotoxicity *in vitro*. The *in vivo* imaging experiment demonstrated that **P2**-KLAK micelles accumulated in the targeted tumor sites by EPR effect. Furthermore, DOX-loaded **P2**-KLAK micelles could more effectively suppressed tumor growth than DOX-loaded **P2** micelles and **P2**-KLAK micelles. We envisioned that the co-delivery of self-assembled KLAK and chemotherapeutic drugs can be applied as effective anti-cancer nano-drugs in the further.

Acknowledgments

This work was supported by the National Basic Research Program of China (973 Program, 2013CB932701), the 100-Talent Program of the Chinese Academy of Sciences, National Natural Science Foundation of China (21374026, 21304023 and 51303036) and Beijing Natural Science Foundation (2132053).

Notes and references

[a] CAS Key Laboratory for Biological Effects of Nanomaterials and Nanosafety, National Center for Nanoscience and Technology (NCNST), Beijing, 100190, China.
[b] School of Chemical Engineering & Technology, Hebei University of Technology, Tianjin, 300130, China.
[c] College of Marine Life Science, Ocean University of China, No. 5 Yushan Road, Qingdao, China.
§ These authors contributed equally to this work.
Corresponding author: wanghao@nanoctr.cn

Electronic Supplementary Information (ESI) available: ^{1}H NMR spectra of copolymers and peptide, in vivo NIR optical imaging. See DOI: 10.1039/b000000x/

References

1. Z. Antosova, M. Mackova, V. Kral and T. Macek, *Trends Biotechnol.*, 2009, **27**, 628-635.
2. E. Zhang, C. Zhang, Y. Su, T. Cheng and C. Shi, *Drug Discov. Today*, 2011, **16**, 140-146.
3. D. Gaspar, A. S. Veiga and M. A. Castanho, *Front. Microbiol.*, 2013, **4**, 294.
4. K. C. Mulder, L. A. Lima, V. J. Miranda, S. C. Dias and O. L. Franco, *Front. Microbiol.*, 2013, **4**, 321.
5. A. A. Kaspar and J. M. Reichert, *Drug Discov. Today*, 2013, **18**, 807-817.
6. M. Góngora-Benítez, J. Tulla-Puche and F. Albericio, *Chem. Rev.*, 2013, **114**, 901-926.
7. F. Schweizer, *Eur. J. Pharmacol.*, 2009, **625**, 190-194.
8. S. Aryal, C.-M. J. Hu and L. Zhang, *ACS Nano*, 2009, **4**, 251-258.
9. M. M. Javadpour, M. M. Juban, W. C. J. Lo, S. M. Bishop, J. B. Alberty, S. M. Cowell, C. L. Becker and M. L. McLaughlin, *J. Med. Chem.*, 1996, **39**, 3107-3113.
10. M. M. Javadpour and M. D. Barkley, *Biochemistry*, 1997, **36**, 9540-9549.
11. C. Polanco Gonzalez, M. A. Nuno Maganda, M. Arias-Estrada and G. del Rio, *Plos One*, 2011, **6**, e21399.
12. P. D. Rakowska, H. Jiang, S. Ray, A. Pyne, B. Lamarre, M. Carr, P. J. Judge, J. Ravi, U. I. M. Gerling, B. Koksch, G. J. Martyna, B. W. Hoogenboom, A. Watts, J. Crain, C. R. M. Grovenor and M. G. Ryadnov, *Proc. Natl. Acad. Sci. USA*, 2013, **110**, 8918-8923.
13. H. M. Ellerby, W. Arap, L. M. Ellerby, R. Kain, R. Andrusiak, G. Del Rio, S. Krajewski, C. R. Lombardo, R. Rao, E. Ruoslahti, D. E. Bredesen and R. Pasqualini, *Nat. Med.*, 1999, **5**, 1032-1038.
14. R. Smolarczyk, T. Cichon, K. Graja, J. Hucz, A. Sochanik and S. Szala, *Acta Biochim. Pol.*, 2006, **53**, 801-805.
15. K. Rege, S. J. Patel, Z. Megeed and M. L. Yarmush, *Cancer Res*, 2007, **67**, 6368-6375.
16. K. Karjalainen, D. E. Jaalouk, C. E. Bueso-Ramos, A. J. Zurita, A. Kuniyasu, B. L. Eckhardt, F. C. Marini, B. Lichtiger, S. O'Brien, H. M. Kantarjian, J. E. Cortes, E. Koivunen, W. Arap and R. Pasqualini, *Blood*, 2011, **117**, 920-927.
17. X. Ma, L. Xi, D. Luo, R. Liu, S. Li, Y. Liu, L. Fan, S. Ye, W. Yang, S. Yang, L. Meng, J. Zhou, S. Wang and D. Ma, *Plos One*, 2012, **7**, e42685.
18. M. Cieslewicz, J. Tang, J. L. Yu, H. Cao, M. Zavaljevski, K. Motoyama, A. Lieber, E. W. Raines and S. H. Pun, *Proc. Natl. Acad. Sci. USA*, 2013, **110**, 15919-15924.
19. L. Hou, X. Zhao, P. Wang, Q. Ning, M. Meng and C. Liu, *Plos One*, 2013, **8**, e53491.
20. J. C. Mai, Z. B. Mi, S. H. Kim, B. Ng and P. D. Robbins, *Cancer Res.*, 2001, **61**, 7709-7712.
21. H. Y. Kim, S. Kim, H. Youn, J. K. Chung, D. H. Shin and K. Lee, *Biomaterials*, 2011, **32**, 5262-5268.
22. B. Law, L. Quinti, Y. Choi, R. Weissleder and C. H. Tung, *Mol. Cancer Ther.*, 2006, **5**, 1944-1949.
23. M. K. Kwon, J. O. Nam, R. W. Park, B. H. Lee, J. Y. Park, Y. R. Byun, S. Y. Kim, I. C. Kwon and I. S. Kim, *Mol. Cancer Ther.*, 2008, **7**, 1514-1522.
24. C. L. Watkins, P. Brennan, C. Fegan, K. Takayama, I. Nakase, S. Futaki and A. T. Jones, *J. Control. Release*, 2009, **140**, 237-244.
25. I. Nakase, S. Okumura, S. Katayama, H. Hirose, S. Pujals, H. Yamaguchi, S. Arakawa, S. Shimizu and S. Futaki, *Chem. Commun.*, 2012, **48**, 11097-11099.
26. K. Li, X.-X. Lv, F. Hua, H. Lin, W. Sun, W.-B. Cao, X.-M. Fu, J. Xie, J.-J. Yu, Z. Li, H. Liu, M.-Z. Han and Z.-W. Hu, *Int. J. Cancer*, 2014, **134**, 692-702.
27. A. J. Marks, M. S. Cooper, R. J. Anderson, K. H. Orchard, G. Hale, J. M. North, K. Ganeshaguru, A. J. Steele, A. B. Mehta, M. W. Lowdell and R. G. Wickremasinghe, *Cancer Res.*, 2005, **65**, 2373-2377.
28. N. Kolevzon, U. Kuflik, M. Shmuel, S. Benhamron, I. Ringel and E. Yavin, *Pharm. Res.*, 2011, **28**, 2780-2789.
29. W.-H. Chen, X.-D. Xu, G.-F. Luo, H.-Z. Jia, Q. Lei, S.-X. Cheng, R.-X. Zhuo and X.-Z. Zhang, *Sci. Rep.*, 2013, **3**, 3468.
30. S. M. Standley, D. J. Toft, H. Cheng, S. Soukasene, J. Chen, S. M. Raja, V. Band, H. Band, V. L. Cryns and S. I. Stupp, *Cancer Res.*, 2010, **70**, 3020-3026.
31. D. J. Toft, T. J. Moyer, S. M. Standley, Y. Ruff, A. Ugolkov, S. I. Stupp and V. L. Cryns, *ACS Nano*, 2012, **6**, 7956-7965.
32. R. H. Zha, S. Sur and S. I. Stupp, *Adv. Healthcare Mater.*, 2013, **2**, 126-133.
33. L. Agemy, D. Friedmann-Morvinski, V. R. Kotamraju, L. Roth, K. N. Sugahara, O. M. Girard, R. F. Mattrey, I. M. Verma and E. Ruoslahti, *Proc. Natl. Acad. Sci. USA*, 2011, **108**, 17450-17455.

34. X. Ma, X. Wang, M. Zhou and H. Fei, *Adv. Healthcare Mater.*, 2013, **2**, 1638-1643.
35. Y. Shamay, L. Adar, G. Ashkenasy and A. David, *Biomaterials*, 2011, **32**, 1377-1386.
36. B. R. Lee, K. T. Oh, Y. T. Oh, H. J. Baik, S. Y. Park, Y. S. Youn and E. S. Lee, *Chem. Commun.*, 2011, **47**, 3852-3854.
37. L. Adar, Y. Shamay, G. Journo and A. David, *Polym. Adv. Technol.*, 2011, **22**, 199-208.
38. A. W. Du and M. H. Stenzel, *Biomacromolecules*, 2014, **15**, 1097-1114.
39. X.-X. Zhang, H. S. Eden and X. Chen, *J. Control. Release*, 2012, **159**, 2-13.
40. D. Polyak, A. Eldar-Boock, H. Baabur-Cohen and R. Satchi-Fainaro, *Polym. Adv. Technol.*, 2013, **24**, 777-790.
41. M. K. Danquah, X. A. Zhang and R. I. Mahato, *Adv. Drug Del. Rev.*, 2011, **63**, 623-639.
42. L. Wang, L.-l. Li, Y.-s. Fan and H. Wang, *Adv. Mater.*, 2013, **25**, 3888-3898.
43. J.-H. Xu, F.-P. Gao, X.-F. Liu, Q. Zeng, S.-S. Guo, Z.-Y. Tang, X.-Z. Zhao and H. Wang, *Chem. Commun.*, 2013, **49**, 4462-4464.
44. L. Wang, L.-L. Li, H. L. Ma and H. Wang, *Chin. Chem. Lett.*, 2013, **24**, 351-358.
45. Y. Liu, L.-L. Li, G.-B. Qi, X.-G. Chen and H. Wang, *Biomaterials*, 2014, **35**, 3406-3415.
46. Y. Liu, F.-P. Gao, D. Zhang, Y.-S. Fan, X.-G. Chen and H. Wang, *J. Control. Release*, 2014, **173**, 140-147.
47. Z.-Y. Qiao, R. Zhang, F. S. Du, D. H. Liang and Z. C. Li, *J. Control. Release*, 2011, **152**, 57-66.
48. Z.-Y. Qiao, F. S. Du, R. Zhang, D. H. Liang and Z. C. Li, *Macromolecules*, 2010, **43**, 6485-6494.
49. Z.-Y. Qiao, J. Cheng, R. Ji, F.-S. Du, D.-H. Liang, S.-P. Ji and Z.-C. Li, *RSC Adv.*, 2013, **3**, 24345-24353.
50. S. Y. Park, H. J. Baik, Y. T. Oh, K. T. Oh, Y. S. Youn and E. S. Lee, *Angew. Chem. Int. Ed.*, 2011, **50**, 1644-1647.
51. E. M. Bachelder, T. T. Beaudette, K. E. Broaders, J. Dashe and J. M. J. Frechet, *J. Am. Chem. Soc.*, 2008, **130**, 10494-10495.
52. X. Huang, X. Jiang, Q. Yang, Y. Chu, G. Zhang, B. Yang and R. Zhuo, *J. Mater. Chem. B*, 2013, **1**, 1860-1868.
53. W. Lin, S. Nie, Q. Zhong, Y. Yang, C. Cai, J. Wang and L. Zhang, *J. Mater. Chem. B*, 2014, **2**, 4008-4020.
54. H. Wang, J. He, M. Zhang, Y. Tao, F. Li, K. C. Tam and P. Ni, *J. Mater. Chem. B*, 2013, **1**, 6596-6607.
55. D. M. Lynn and R. Langer, *J. Am. Chem. Soc.*, 2000, **122**, 10761-10768.
56. D. M. Lynn, M. M. Amiji and R. Langer, *Angew. Chem. Int. Ed.*, 2001, **40**, 1707-1710.
57. X. Deng, N. Zheng, Z. Song, L. Yin and J. Cheng, *Biomaterials*, 2014, **35**, 5006-5015.
58. J. Ko, K. Park, Y. S. Kim, M. S. Kim, J. K. Han, K. Kim, R. W. Park, I. S. Kim, H. K. Song, D. S. Lee and I. C. Kwon, *J. Control. Release*, 2007, **123**, 109-115.
59. W. Song, Z. Tang, M. Li, S. Lv, H. Yu, L. Ma, X. Zhuang, Y. Huang and X. Chen, *Macromol. Biosci.*, 2012, **12**, 1375-1383.
60. J. Chen, X. Qiu, J. Ouyang, J. Kong, W. Zhong and M. M. Q. Xing, *Biomacromolecules*, 2011, **12**, 3601-3611.
61. S. Tang, Q. Yin, Z. Zhang, W. Gu, L. Chen, H. Yu, Y. Huang, X. Chen, M. Xu and Y. Li, *Biomaterials*, 2014, **35**, 6047-6059.
62. Z.-Y. Qiao, S.-L. Qiao, G. Fan, Y.-S. Fan, Y. Chen and H. Wang, *Polym. Chem.*, 2014, **5**, 844-853.
63. Z. Duan, Y. Gao, Z.-Y. Qiao, G. Fan, Y. Liu, D. Zhang and H. Wang, *J. Mater. Chem. B*, 2014, **2**, 6271-6282.
64. A. Akinc, D. G. Anderson, D. M. Lynn and R. Langer, *Bioconjugate Chem.*, 2003, **14**, 979-988.
65. D. G. Anderson, W. D. Peng, A. Akinc, N. Hossain, A. Kohn, R. Padera, R. Langer and J. A. Sawicki, *Proc. Natl. Acad. Sci. USA*, 2004, **101**, 16028-16033.
66. S. W. Provencher and J. Gloeckner, *Biochemistry*, 1981, **20**, 33-37.
67. I. H. M. van Stokkum, H. J. W. Spoelder, M. Bloemendal, R. van Grondelle and F. C. A. Groen, *Anal. Biochem.*, 1990, **191**, 110-118.
68. F. M. Winnik, *Chem. Rev.*, 1993, **93**, 587-614.
69. H. Wu, L. Zhu and V. P. Torchilin, *Biomaterials*, 2013, **34**, 1213-1222.
70. E. S. Lee, K. T. Oh, D. Kim, Y. S. Youn and Y. H. Bae, *J. Control. Release*, 2007, **123**, 19-26.
71. X. N. Huang, F. S. Du, J. Cheng, Y. Q. Dong, D. H. Liang, S. P. Ji, S. S. Lin and Z. C. Li, *Macromolecules*, 2009, **42**, 783-790.
72. Z.-Y. Qiao, R. Ji, X.-N. Huang, F.-S. Du, R. Zhang, D.-H. Liang and Z.-C. Li, *Biomacromolecules*, 2013, **14**, 1555-1563.
73. O. A. Kucherak, S. Oncul, Z. Darwich, D. A. Yushchenko, Y. Arntz, P. Didier, Y. Mély and A. S. Klymchenko, *J. Am. Chem. Soc.*, 2010, **132**, 4907-4916.
74. J. J. Green, R. Langer and D. G. Anderson, *Acc. Chem. Res.*, 2008, **41**, 749-759.
75. M. E. Davis, Z. Chen and D. M. Shin, *Nat. Rev. Drug Discov.*, 2008, **7**, 771-782.
76. U. Mayerhoeffer, B. Fimmel and F. Würthner, *Angew. Chem. Int. Ed.*, 2012, **51**, 164-167.

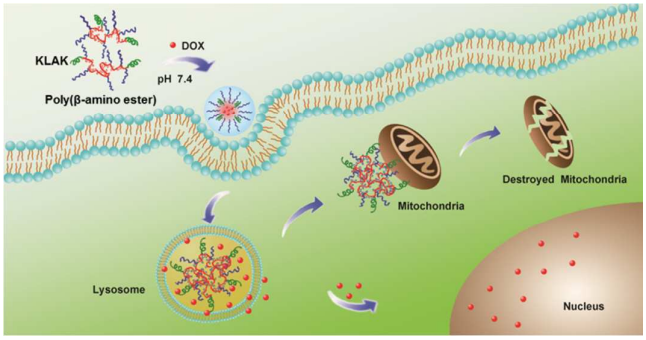

DOX-encapsulated self-assembled micelle formation by cytotoxic peptide conjugated poly(β-amino ester)s for synergistic cancer chemotherapy